

# Myonecrosis Induced by Rattlesnake Venom

## *An Electron Microscopic Study*

John M. Stringer MD, Robert A. Kainer DVM, MS and Anthony T. Tu PhD

The myonecrotic effect of rattlesnake (*Crotalus viridis viridis*) venom on mouse skeletal muscle was studied. The biceps femoris muscle was examined with the electron microscope after one-fourth the LD<sub>50</sub> of the crude venom was injected into the gracilis and semimembranosus muscles. Focal areas of myonecrosis were abundant. Injured fibers contained dilated sarcoplasmic reticulum, disoriented, coagulated myofilamentous components and condensed, rounded and enlarged mitochondria. The external lamina and sarcolemma remained intact in many fibers. Hemorrhage was apparent in the endomysial connective tissue, and hemolysis was discernible. In areas where the erythrocytes were tightly packed between the muscle fibers, there was disruption of the external lamina and sarcolemma. Degeneration of the fibers in these areas was pronounced. These findings correlate well with the breakdown of muscle fibers by various methods described in the literature. Myonecrosis induced by snake venom may serve as a useful model for studying muscle necrosis because of its rapid onset and relative ease of induction. (Am J Pathol 67:127-140, 1972)

SNAKEBITE IS NOT UNCOMMON throughout most of the world, predominantly in the tropical areas. Deaths due to snakebite have been estimated to be between 30,000 and 40,000 annually.<sup>1</sup> In the United States, it has been estimated that, of the 6000 individuals bitten each year, 15 cases are fatal.<sup>2</sup> No accurate statistics are available for snakebite, because no one can accurately assemble all the cases. However, a good record was kept by the Venomous Snakebite Committee of the Florida State Board of Health. The committee reported 382 verified and completed records of snakebite.<sup>3</sup> Of this number, 168 were inflicted by pigmy rattlesnake (*Sistrurus miliarius*) and 71 by larger rattlesnakes (*Crotalus*). Cottonmouth moccasins (*Agkistrodon piscavoris*) accounted for 69 bites, copperheads (*Agkistrodon contortrix*) for 4, coral snakes (*Micrurus*) for 14 and unidentified venomous snakes for 56. Some snakebite victims survive, but sustain permanent tissue damage that may extend into the muscle, tendons and cartilage.<sup>4,5</sup> The destruction of tissue, with possible disfunction or complete loss

---

From the Department of Anatomy and Department of Biochemistry, Colorado State University, Fort Collins, Colo.

Supported by grant 5R01 GM-15591 and 5R01 FD-00014 from the US Public Health Service and Career Development Award 5K04 GM-41786 from the National Institutes of Health (to A. T. Tu).

Accepted for publication October 7, 1971.

Address reprint requests to Dr. Anthony T. Tu, Department of Biochemistry, Colorado State University, Fort Collins, Colo 80521.

of a body part, is an important factor in snakebite cases, since, in many cases, the use of antivenin does not prevent histolysis unless it is injected minutes after the bite.<sup>6,7</sup>

Most crotaline venoms produce hemorrhage and myonecrosis simultaneously upon envenomation.<sup>8</sup> Many cases of myonecrosis after envenomation by snake venom have been reported.<sup>6,9,10</sup>

A variety of toxins produce myonecrosis. The objective of this study was to determine if the myonecrosis produced by *Crotalus viridis viridis* (prairie rattlesnake) venom was similar to that reported to occur by other mechanisms—*ie*, ischemia due to cold, the drug plasmocid, cobra venom, *Clostridium perfringens* toxin and coxsackie virus.

### Materials and Methods

Twenty-four Swiss white mice served as experimental subjects. Eight animals were used in three separate experiments. Six mice were injected intramuscularly in the medial aspect of the left thigh (gracilis and semimembranosus muscles) with 20  $\mu$ g of crude *C viridis viridis* venom (Ross Allen's Reptile Institute, Silver Springs, Fla) dissolved in 0.1 ml physiologic saline (PSS). Two control animals were injected similarly with 0.1 ml PSS. All animals were killed by cervical dislocation 3 hours after injection. The tissue was removed from the lateral aspect of the injected thigh (biceps femoris muscle) to avoid areas that might have been damaged by the needle. The excised tissue was fixed in 5% glutaraldehyde in Millonig's phosphate buffer, pH 7.2, for 5 hours at 10 C; then it was fixed secondarily for 1 hour in 2% osmium tetroxide in Millonig's phosphate buffer, pH 7.2. After dehydration in a graded series of ethanol, the tissue was embedded in Epon 812.<sup>11</sup> One-micron sections stained with toluidine blue O<sup>12</sup> were used for light microscopic observations of necrotic foci. Thin sections were cut on a Sorvall MT-2 ultramicrotome. The sections were picked up on uncoated 200-mesh copper grids and stained with uranyl acetate and lead citrate.<sup>13</sup> Observations were made with a Zeiss EM 9A or RCA EMU 3F electron microscope.

### Results

#### Control Muscle

Gross examination of the killed control animals revealed no lesions except for an occasional hemorrhagic area at the penetration site of the needle. Tissue from the control animals had all the fine structural aspects of skeletal muscle as described in the literature.<sup>14,17</sup> There were thin actin filaments on either side of the thick myosin filaments with cross bridges between the two filament types. The Z lines were in register with one another. The A band, H band, I band and M lines were present in longitudinal sections of the skeletal muscle. The triad was located at the Z-line complex and the sarcotubular system was comprised of flattened cisternae. Moderate numbers of mitochondria were tightly packed at various locations between the myofibrils and

near the nuclei. Glycogen granules were scattered throughout the muscle fibers in moderate amounts, with the highest concentration near the triads and nuclei. The external lamina closely paralleled the uninterrupted plasma membrane as it encircled the muscle fiber. The elongated, hypolemmal nuclei were characteristic of glutaraldehyde-fixed nuclei. The sarcoplasm was relatively scant as the organelles were in close apposition to one another with no large areas devoid of organelles (Fig 1).

#### *Experimental Muscle*

The experimental animals had extensive ventral hemorrhage and edema extending from the gracilis muscle to the pectoralis muscles on either side of the midline.

Upon examination with the light microscope, hemorrhage was apparent between fibers, and focal areas of myonecrosis were observed.

Electron microscopic observations disclosed various levels of degeneration among muscle fibers. Relatively intact fibers were intermixed with fibers undergoing degeneration.

The first indication of degeneration was the obvious dilatation of the longitudinal sarcotubular cisternae. The characteristic, flattened vacuoles swelled and became more prominent as degeneration progressed. Vacuoles lying deep to the plasma membrane became swollen and many possessed myeloid figures (Fig 2). During the early dilatation of the sarcoplasmic reticulum, it retained some organization (Fig 3) but became more randomly scattered as the swelling increased until, in some instances, the cell was nearly 30% vacuoles (Fig 4). As the degeneration progressed, the vacuoles became smaller and fewer until they were mostly obliterated by the fibrils (Fig 5 and 9).

The T system remained intact throughout most of the degenerative process (Fig 2, 3, and 9). In the later stages, transverse tubules could not be readily identified but they might have been present as small, randomly scattered vesicles (Fig 7 and 9).

With the increase in vacuole size and distribution, the myofibrils appeared to atrophy (Fig 4 and 6). The first breakdown in the striated appearance occurred with the disappearance of the H band and its M line (Fig 3 and 11). The Z line retained the integrity and orientation of the myofibril. After the Z line broke down, the actin filaments became less apparent. The myosin filaments appeared thicker and less discrete (Fig 6). As degeneration progressed, myofibrillar organization was lost until the protein became long strands containing many fine filaments and lacking their complete linear

alignment (Fig 7). Degeneration of myofibrils appeared to be complete when they became an amorphous coagulation of light and dark masses (Fig 9).

Degeneration of the mitochondria seemed somewhat slower than that of other organelles. The mitochondrial size and/or the number of cristae increased, probably due to the metabolic activity (Fig 3 and 5). Extreme mitochondrial degeneration was not apparent before the fibrillar components broke down (Fig 2). As the mitochondrial degeneration progressed, the cristae ruptured and the mitochondrial fragment became surrounded by small vacuoles (Fig 7). Some ruptured mitochondria contained a flocculant material (Fig 10).

In early stages of degeneration, the nuclei became pyknotic with a dilatation of the double nuclear membrane. As the degeneration progressed, the chromatin became densely clumped around the periphery of the nucleus and made up the greatest portion of the nucleus (Fig 11).

The external lamina remained intact throughout most of the degenerative process; only in the latter stages was it destroyed (Fig 8 and 11). Destruction of the plasma membrane closely paralleled that of the external lamina. Some breaks in the plasma membrane were seen in degenerating cells (Fig 4, 7 and 11).

Glycogen levels appeared to be at nearly normal levels in early stages of degeneration, but as the dilatation of the sarcoplasmic reticulum increased, the amount of glycogen was diminished.

In areas of extreme hemorrhage (Fig 12) where the erythrocytes were closely packed in the endomysial space, various changes were seen. The sarcolemma was broken, and myofibrillar degeneration was apparent. The mitochondria were swollen and tightly packed under the sarcolemma (Fig 12). There were many areas where the erythrocytes lay closely apposed to myofilaments and mitochondria (Fig 13). Hemolysis also occurred in these areas (Fig 8 and 13). A diagrammatic summary of these events is presented in Fig 14.

## Discussion

Myonecrosis of striated muscle has been studied by means of the light microscope for some time. The types of injuries that develop as a result of various noxious agents vary from minimal cloudy swelling of the sarcoplasm to total necrosis of the muscle fiber. Ischemia or injection of chemical agents into muscle results in necrosis with preservation of a well-marked refractile Z line forming discs or short segments. Heat, cold or other physical trauma usually result in fragmentation or shredding of the muscle fibers.<sup>18,19</sup>

Stenger *et al* observed ischemic skeletal muscle after intervals of 6½, 24 and 48 hours. Myofibrillar integrity was maintained as late as 24 hours after ischemia. However, after a 48-hour interval, degeneration of the I band and Z line was noted with striking preservation of the A band, H band and M line. Glycogen diminished in the skeletal muscle fibers in the first 24 hours.<sup>20</sup>

The most marked alterations in the ultrastructure of diaphragm muscle after hemorrhagic shock were seen in the mitochondria. They swelled and ruptured prior to the swelling of the other intracellular organelles.<sup>21</sup>

After congestive cardiomyopathy,<sup>22</sup> alterations in the Z line were the primary defect. The most severe lesion was a complete disruption of myofibrils adjacent to an irregular Z line. This consisted of an unstructured mass containing irregularly arranged intercalated discs.

In necrosis induced by cold, Price *et al* observed the disappearance of the striations at the I and H bands.<sup>23</sup> The mitochondria were swollen and their cristae disintegrated. The plasma membrane was broken in places, but the external lamina remained to constitute the sarcolemmal tube. The nuclear chromatin was clumped at the periphery, and the outer nuclear membranes contained blebs. The myofibrils became a uniform mass of thin filaments and eventually changed into finely granular debris.

In necrosis induced by plasmocid, a drug related to the antimalarial drugs primaquine and pamaquine, an early focal dissolution of the I-band filaments and the Z line, with eventual disappearance of both these structures, was described; yet the A band was remarkably stable.<sup>24</sup> The sarcoplasmic reticulum was observed to be dilated while the T system was not changed. D'Agostino used larger doses of plasmocid and detected focal loss of the myofilaments including the A band.<sup>25</sup> Aggregates of vesicles under the sarcolemma were also observed.

Strunk *et al* described the myonecrotic effect of *Clostridium perfringens* toxin.<sup>26</sup> The initial lesion was the disruption of the plasma membrane. They believe the degeneration of the myofilaments, mitochondria, sarcoplasmic reticulum and nucleus to be secondary manifestations of lesions of the plasma membrane.

Muscle degeneration due to infection of muscles in suckling mice with coxsackie A4 virus was reported by Harrison *et al*.<sup>27</sup> They noted myofibrillar degeneration with swollen and distorted mitochondria. The nuclei were crenated and pyknotic, with margination and condensation of chromatin. The nuclear membranes had wide separations.

Myocardial damage induced by scorpion venom varied with means

of injection. Swollen mitochondria, focal destruction of myofibrils and sarcoplasmic reticulum resulted, but the cell membrane remained intact.<sup>28</sup>

Trevino reported loss of myofibrillar organization and clumping of material after *Crotalus atrox* envenomation of porcine muscle.<sup>29</sup> He postulated that this material may be precipitated protein globules. He reported irregularly shaped erythrocytes with a dark, granular substance adhering to the plasma membrane and thought this material might be a conjugation of venom with phospholipids.

Myonecrosis induced by cobra venom<sup>30</sup> produced complete degeneration of muscle fibers. The sarcoplasmic reticulum was dilated and myofibrils were disoriented, resulting in an amorphous electron-dense mass. Complete lysis of the cell was observed within 1 hour after the venom was injected.

In many of the aforementioned experimental lesions,<sup>23-26</sup> there was minimal damage to the plasma membrane and consequently to the T system. In the case of *Clostridium perfringens* toxin, there was measurable damage to the plasma membrane, but no reference was made to the T system. We have demonstrated that although the sarcoplasmic reticulum was very disorganized and swollen in muscle fibers damaged by venom from *C. viridis viridis*, a well-organized and cohesive T system was still maintained (Fig 4, 5 and 10).

It is quite evident that the sarcoplasmic reticulum is more susceptible to the effects of injurious substances than is the T system.<sup>19,31</sup>

Augustyn *et al*<sup>32</sup> correlated swollen mitochondria having broken limiting membranes and cristae with respiratory inhibition that occurred when isolated mitochondria from rat liver were subjected to either crude venom from water moccasins or purified phospholipase A obtained from the venom.

If this correlation is true, we might assume that the mitochondria are metabolically active throughout most of the myofibrillar degenerative process (Fig 4, 5 and 9). The mitochondria are swollen and condensed but still maintain structural integrity, indicating that respiration may still be in progress.

Retention of the Z-line structure may be indicative of its different protein complement (tropomyosin) or the very tight interwoven meshwork of its construction<sup>32</sup> that prohibits early penetration by the toxins.

Cytochemical and biochemical studies need to be performed before many of these observations can be fully understood. However, snake venom-induced myonecrosis may conceivably provide an excellent model for studying the mechanisms of muscle degeneration.

## References

1. Swaroop S, Grab B: The snakebite mortality problem in the world, Venoms. Edited by EE Buckley, N Porges. Washington DC, American Association for the Advancement of Science, 1956
2. Parrish HM, Silberg SL, Grolldner JC: Snakebite: a pediatric problem. *Clin Pediatr* 4:237-241, 1965
3. Andrews CE, Dees JE, Edwards RO: Venomous snakebite in Florida. *J Fla Med Assoc* 55:308-316, 1968
4. Emery JA, Russell FE: Lethal and hemorrhagic properties of some North American snake venoms, *Venomous and Poisonous Animals and Noxious Plants of the Pacific Region*. Edited by HL Keegan, WJ MacFarlane. New York, Pergamon Press, 1963, pp 409-414
5. McCollough ND, Gennaro JF: Evaluation of venomous snakebite in the southern United States from parallel clinical and laboratory investigations: development of treatment. *J Fla Med Assoc* 40:959-967, 1963
6. Stahnke HL: *The Treatment of Venomous Bites and Stings*. Tempe, Ariz, Bureau Publications of Arizona State University, 1966
7. McCollough ND, Gennaro JF: Treatment of venomous snakebite in the United States. *Clin Toxicol* 3:483-500, 1970
8. Tu AT: The mechanism of snake venom actions: rattlesnakes and other crotalids. *The Pathophysiological Actions of Several Biological Poisons*. Edited by L Simpson. New York, Plenum Press, 1971, pp 87-109
9. Tenery JH, Koefoot RR: Snakebite. *Plast Reconstr Surg* 15:483-488, 1955
10. Abalos JW, Pirotsky I: Venomous Argentine serpents ophidism and snake antivenin,<sup>4</sup> pp 363-371
11. Luft JH: Improvements in epoxy resin embedding methods. *J Biophys Biochem Cytol* 9:409-414, 1961
12. Lynn JA: Rapid toluidine blue staining of Epon-embedded and mounted "adjacent" sections. *Am J Clin Pathol* 44:57-58, 1965
13. Fahmy A: An extemporaneous lead citrate stain for electron microscopy, *Proceedings of Electron Microscopy Society of America*. Baton Rouge, La, Claitor's Book Store, 1969, pp 148-149
14. Huxley HE: The contraction of muscle. *Sci Am* 199:67-82, 1958
15. *Idem*: The mechanism of muscular contraction. *Sci Am* 213:18-27, 1965
16. Bennett HS: The structure of striated muscle as seen in the electron microscope, *The Structure and Function of Muscle*. Vol 1. Edited by GH Bourne. New York, Academic Press Inc, 1960, pp 136-182
17. Porter KR, Palade GE: Studies on the endoplasmic reticulum. III. Its form and distribution in striated muscle cells. *J Biophys Biochem Cytol* 3:269-300
18. Adams RD, Denny-Brown D, Pearson CM: *Diseases of Muscle: A Study in Pathology*. Second edition. New York, Harper & Row, 1962
19. Pellegrino C, Franzini-Armstrong C: Recent contributions of electron microscopy to the study of normal and pathological muscle, *Int Rev Exp Pathol* 7:139-226, 1969
20. Stenger RJ, Spiro D, Scully RE, Shannon JM: Ultrastructural and physiological alterations in ischemic skeletal muscle. *Am J Pathol* 40:1-20, 1962
21. Holden WD, DePalma RG, Drucker WR, McKalen A: Ultrastructural

- changes in hemorrhagic shock; electron microscopic study of liver, kidney and striated muscle cells in rats. *Ann Surg* 162:517-536, 1965
22. Rodin HE, Harris LC, Nghiem QX: Idiopathic, nonobstrusive cardiomyopathy. *Arch Pathol* 91:62-69, 1971
  23. Price HM, Pease DC, Blumberg JM: Ultrastructural alterations in skeletal muscle fibers injured by cold: the acute degenerative changes. *Lab Invest* 13:1265-1278, 1964
  24. Price HM, Pease DC, Pearson CM: Selective actin filament and Z band degeneration induced by plasmocid: an electron microscopic study. *Lab Invest* 11:549-562, 1962
  25. D'Agostino AN: An electron microscopic study of skeletal and cardiac muscle of the rat poisoned by plasmocid. *Lab Invest* 12:1060-1071, 1963
  26. Strunk SW, Smith CW, Blumberg JM: Ultrastructural studies on the lesion produced in skeletal muscle fibers by crude type A *Clostridium perfringens* toxin and its purified alpha fractions. *Am J Pathol* 50:89-108, 1967
  27. Harrison AK, Murphy FA, Gary GW Jr: Ultrastructural pathology of coxsackie A4 virus infection of mouse striated muscle. *Exp Mol Pathol* 14:30-42, 1971
  28. Yarom R, Braun K: Electron microscopic studies of the myocardial changes produced by scorpion venom injections in dogs. *Lab Invest* 24:21-30, 1971
  29. Trevino GS: Pathologic effects of the venoms of *Crotalus atrox* and *Naja naja* in pigs. PhD thesis. East Lansing, Michigan State University, 1968
  30. Stringer JM, Kainer RA, Tu AT: Ultrastructural studies of myonecrosis induced by cobra venom in mice. *Toxicol Appl Pharmacol* 18:442-450, 1971
  31. Fahimi HD, Cotran RS: Permeability studies in heat induced injury of skeletal muscle using lanthanum as fine structural tracer. *Am J Pathol* 62:143-157, 1971
  32. Augustyn JM, Parsa B, Elliott WB: Structural and respiratory effects of *Agkistrodon piscivorus* phospholipase A on rat liver mitochondria. *Biochim Biophys Acta* 197:185-196, 1970
  33. MacDonald RD, Engel AG: Observations on organization of Z-disk components and on rod bodies of Z-disk origin. *J Cell Biol* 48:431-437, 1971

The authors wish to thank Mr. Dennis Giddings for the drawings and the Electron Microscopy Training Laboratory for the facilities to do this study.



*[Illustrations follow]*

### Legends for Figures

**Fig 1**—Electron micrograph of a portion of a skeletal muscle fiber from a control animal. *Z* indicates Z line; *A*, A band; *I*, I band; *H*, H band; *M*, M line; *sr*, sarcoplasmic reticulum; *mi*, mitochondria; *black arrows*, transverse tubules or T system ( $\times 9000$ ).

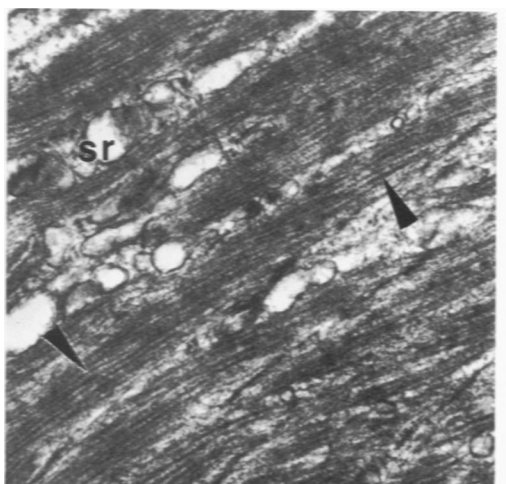
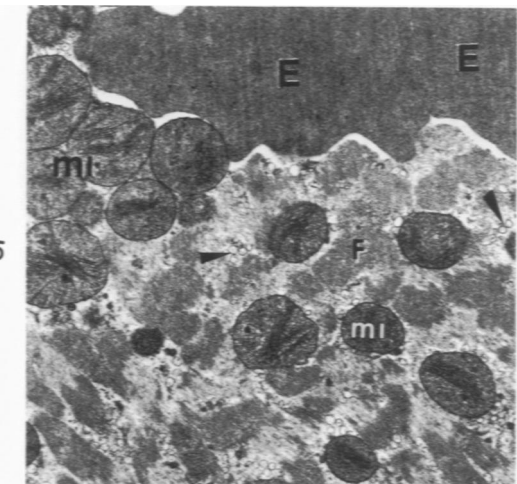
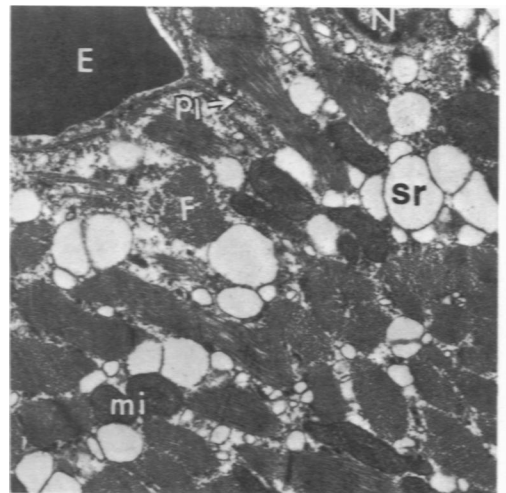
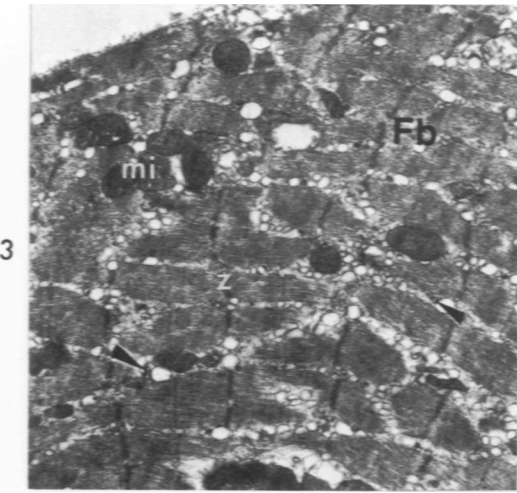
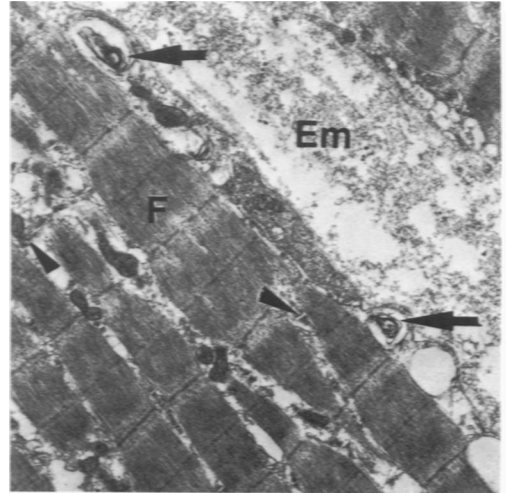
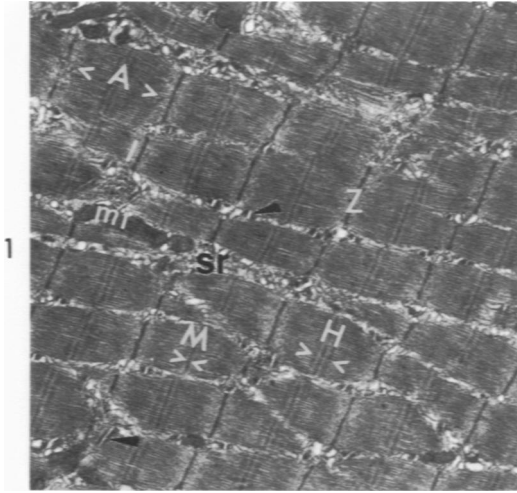
**Fig 2**—The degenerate fiber at lower left contains many large vacuoles under the plasma membrane, some of which contain myeloid figures (*long arrows*). The separation and atrophy of the myofibrils is apparent in this fiber when compared to the fiber in Fig 1. *Short arrows* indicate transverse tubules; *Em*, endomysial space; *F*, myofilaments ( $\times 9000$ ).

**Fig 3**—Electron micrograph of venom-injected skeletal muscle. The proliferated sarcoplasmic reticulum can be seen as many small vesicles between the myofibrils (*Fb*). The myofibrils are smaller and the H band and M line are less dense than in the control muscle. The mitochondria (*mi*) are enlarged and irregularly shaped. The transverse tubules still appear intact. *Z* indicates Z line ( $\times 9000$ ).

**Fig 4**—Portion of a degenerated skeletal muscle fiber with extreme dilation of the sarcoplasmic reticulum (*sr*). The myofibrils are smaller and the interfibrillar space is more abundant than in the control muscle. Myofilaments (*F*) can be resolved at this stage of degeneration. The plasma membrane (*PL*) is broken at irregular intervals and the external lamina appears granular. The nucleus (*N*) is pyknotic and lacks a distinct double membrane. *E* indicates erythrocyte; *mi*, mitochondria ( $\times 9000$ ).

**Fig 5**—In this electron micrograph of venom-injected skeletal muscle, the mitochondria (*mi*) are greatly enlarged and their cristae are abnormally arranged. The myofibrils are closely packed together and lack their cross-striated appearance. Individual myofilaments (*F*) can be resolved. The vesicles of the sarcoplasmic reticulum (*arrows*) appear fewer and smaller than those in Fig 6. The transverse tubules are difficult to identify positively. *E* indicates erythrocytes ( $\times 9000$ ).

**Fig 6**—This degenerate muscle fiber lacks the characteristic cross striations. The thick myosin filaments (*arrows*) are present but disoriented. The thin actin filaments are not discernible. The sarcoplasmic reticulum (*sr*) is dilated ( $\times 28,500$ ).



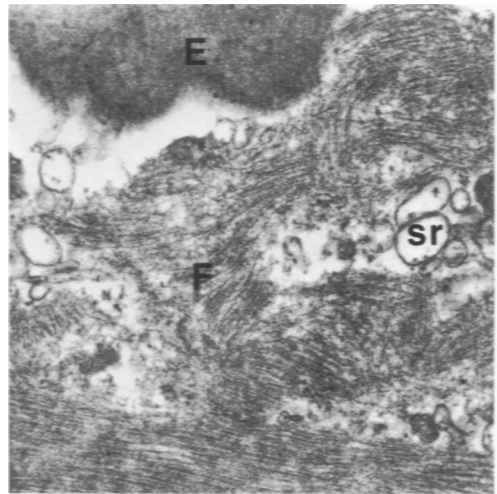
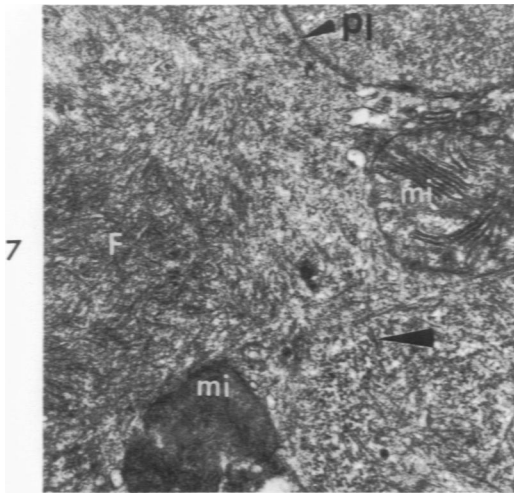


**Fig 7**—Portion of a venom-injected skeletal muscle fiber. The degenerate mitochondria (*Mi*) and disoriented meshwork of myofilaments (*F*) can be seen. Some of the small vesicles (*arrows*) may be remnants of the transverse tubules. *PL* indicates plasma membrane ( $\times 21,600$ ). **Fig 8**—High-magnification electron micrograph of venom-injected skeletal muscle with no plasma membrane or external lamina between the fiber and the erythrocyte (*E*). The myofilaments (*F*) and sarcoplasmic reticulum (*sr*) are in irregular array. The erythrocyte is hemolyzed ( $\times 28,500$ ).

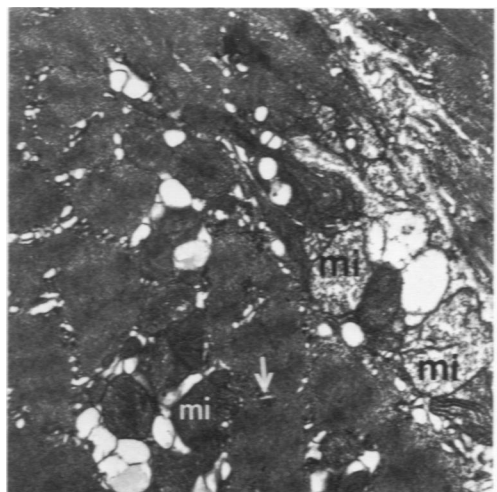
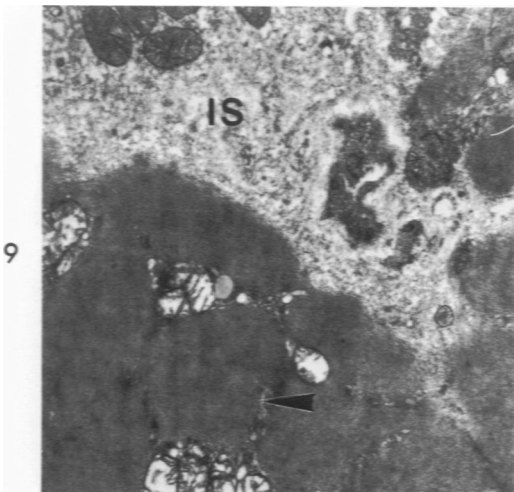
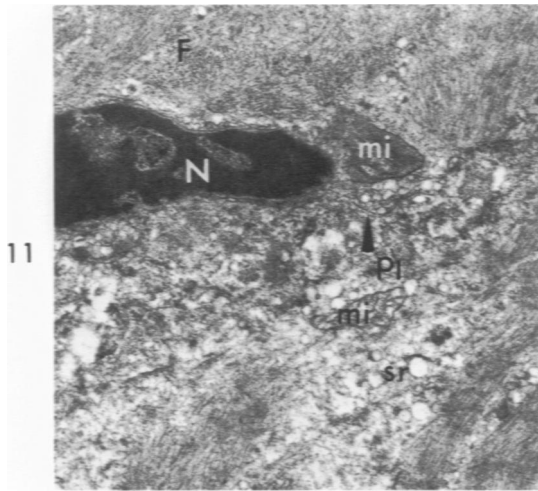
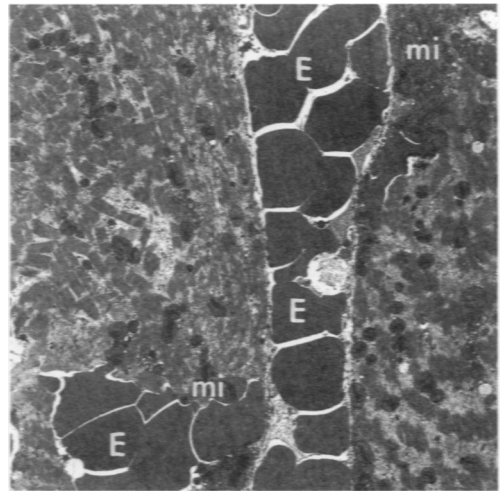


**Fig 9**—In this damaged muscle fiber, the myofilaments have precipitated into an amorphous mass. The filamentous structure is no longer evident, and the mitochondria within it are swollen with fewer, shorter cristae. The intrafibrillar space (*IS*) is greatly increased, the mitochondria in this area are more intact. *Arrows* indicate transverse tubules ( $\times 7950$ ). **Fig 10**—This experimental muscle fiber contains many degenerate mitochondria (*mi*). The mitochondria at the right center of the micrograph contain a flocculant material. Glycogen granules can be seen as black dots in the areas near the mitochondria. *Arrows* indicate transverse tubules ( $\times 9000$ ).



11



12

**Fig 11**—Electron micrograph of necrotic skeletal muscle. The upper fiber contains a pyknotic nucleus (*N*) and disoriented myofilaments (*F*). The lower cell contains disrupted sarcoplasmic reticulum (*sr*) and degenerate mitochondrion (*mi*). The myofibrillar striations are faintly visible in the fibrils in the lower right portion of this fiber. The plasma membrane (*PL*) and external lamina are interrupted at various intervals ( $\times 11,600$ ). **Fig 12**—Low-magnification electron micrograph of venom-injected skeletal muscle. Interfibrillar hemorrhage is prominent along with swollen mitochondria (*mi*) and disruption of the integrity of the myofibrils. *E* indicates erythrocytes ( $\times 2600$ ).

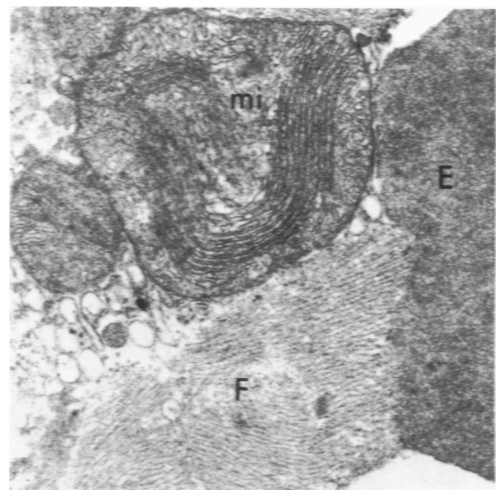


**Fig 13**—Electron micrograph showing the relationship between the damaged fibers and the erythrocytes. In areas of extreme hemorrhage (Fig 12), the erythrocytes were in close apposition to the muscle fibers with no plasma membrane or external lamina separating them. The myofilaments (*F*) seemed to fuse directly with the hemolyzed erythrocyte (*E*). Mitochondria indicated by *mi* ( $\times 28,500$ ).

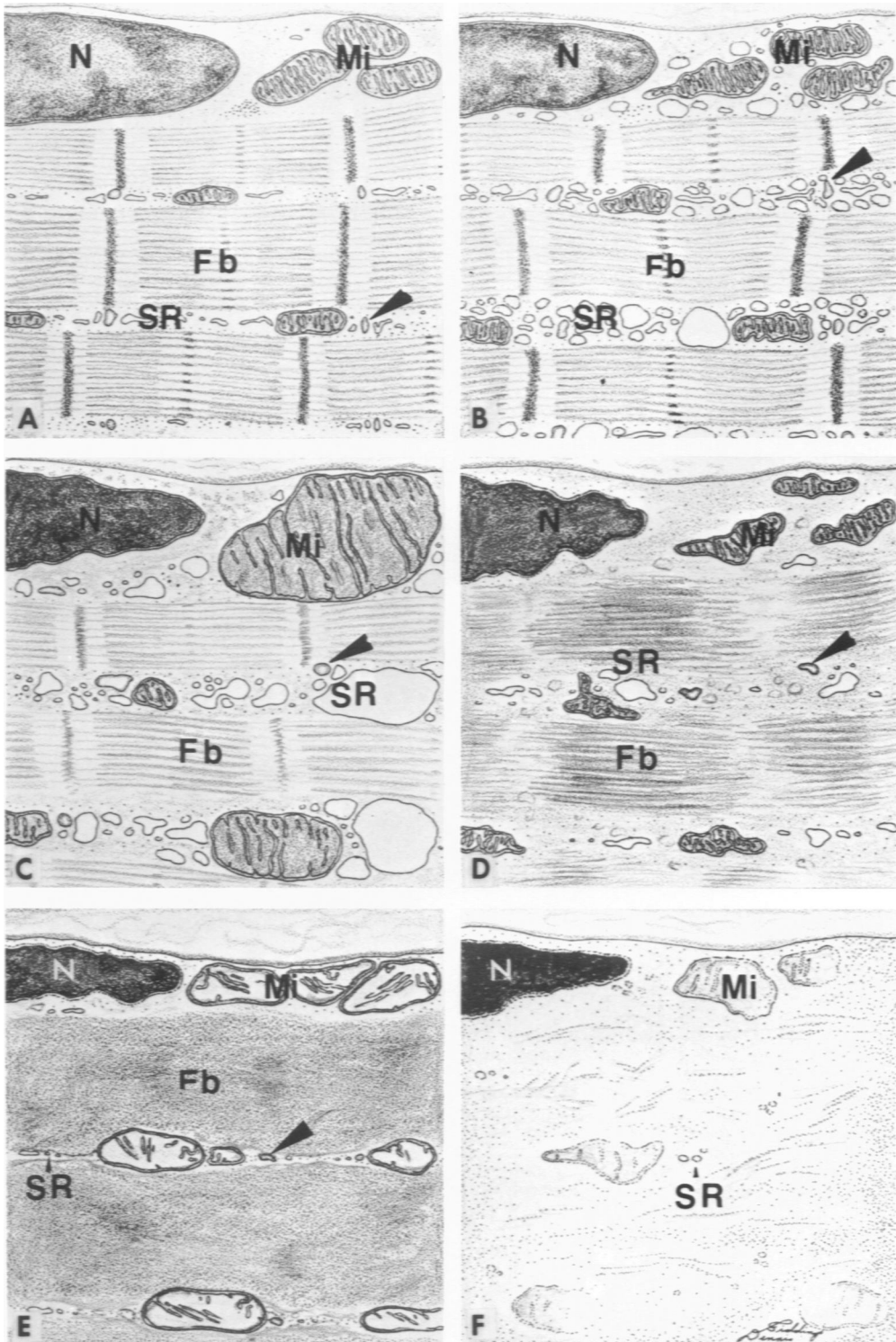


**Fig 14**—Diagrammatic representation of myonecrosis after rattlesnake envenomation. **A** depicts a normal fiber and **F** is that same fiber 3 hours after venom injection. All the sequences shown above can be seen in the electron micrographs presented in the text. **N** indicates nucleus; **mi**, mitochondria; **sr**, sarcoplasmic reticulum; **Fb**, myofibrils; **arrows**, transverse tubules.